

Hund's superconductor Li(Fe,Co)AsH. Miao^{1,*}, Y. L. Wang^{2,*}, J.-X. Yin^{3,*}, J. Zhang¹, S. Zhang³, M. Z. Hasan^{3,4,5,6}, R. Yang⁷, X. C. Wang^{8,9,10}, C. Q. Jin^{8,9,10}, T. Qian^{8,10}, H. Ding^{8,9,10}, H.-N. Lee¹ and G. Kotliar^{11,2}¹Materials Science and Technology Division, Oak Ridge National Laboratory, Oak Ridge, Tennessee 37831, USA²Condensed Matter Physics and Materials Science Department, Brookhaven National Laboratory, Upton, New York 11973, USA³Laboratory for Topological Quantum Matter and Advanced Spectroscopy (B7), Department of Physics, Princeton, New Jersey 08544, USA⁴Princeton Institute for the Science and Technology of Materials, Princeton University, Princeton, New Jersey 08540, USA⁵Materials Sciences Division, Lawrence Berkeley National Laboratory, Berkeley, California 94720, USA⁶Quantum Science Center, Oak Ridge, Tennessee 37931 USA⁷Laboratorium für Festkörperphysik ETH-Zürich, 8093 Zürich, Switzerland⁸Beijing National Laboratory for Condensed Matter Physics, Institute of Physics, Chinese Academy of Sciences, Beijing 100190, China⁹School of Physical Sciences, University of Chinese Academy of Sciences, Beijing 100190, China¹⁰Songshan Lake Materials Laboratory, Dongguan, Guangdong, 523808, China¹¹Physics and Astronomy Department, Rutgers University, Piscataway, New Jersey 08854, USA

(Received 23 November 2020; accepted 25 January 2021; published 10 February 2021)

We combine transport, angle-resolved photoemission spectroscopy, and scanning tunneling spectroscopy to investigate several low-energy manifestations of the Hund's coupling in a canonical FeSC family Li(Fe,Co)As. We determine the doping dependence of the coherent-incoherent crossover temperature and the quasiparticle effective mass enhancement in the normal state. Our tunneling spectroscopy result in the superconducting state supports the idea that superconductivity emerging from Hund's metal state displays a universal maximal superconducting gap vs transition temperature ($2\Delta_{\max}/k_B T_c$) value, which is independent of doping level and T_c .

DOI: [10.1103/PhysRevB.103.054503](https://doi.org/10.1103/PhysRevB.103.054503)**I. INTRODUCTION**

A decade after the first discovery of the high- T_c iron-based superconductors (FeSCs), the pairing mechanism and the interplay between the normal and superconducting state in these materials remain elusive [1–3]. While the phase diagram of the FeSCs shares some similarities with the cuprate high- T_c superconductors, FeSCs are multiorbital semimetals rather than doped Mott insulators with an effective single orbital [4]. The increased orbital degree of freedom is found to qualitatively change the underlying electronic dynamics [5,6]. In particular, dynamical mean-field theory (DMFT) studies have shown that strong electron-electron correlations in the FeSCs originate from the interorbital Hund's coupling, J_H , rather than the on-site intraorbital Coulomb interaction, U [7–15]. Consequently, FeSCs are often dubbed as Hund's metals [9,12].

Evidence of Hund's metals has been found in the paramagnetic state (PM) of several FeSC families, including doping-dependent effective mass [13], and orbital differentiations [16–19]. More recently, theoretical analysis of the Hundness on superconductivity is linked to the ratio $2\Delta_{\max}/k_B T_c$ in FeSCs [20,21], where Δ_{\max} is the largest superconducting gap in the momentum space. Despite this important experimental and theoretical progress, justification of Hund's superconductivity requires synergetic transport and

spectroscopy studies of the Hundness that covers the whole superconducting dome as well as their normal state. Here, using transport, angle-resolved photoemission spectroscopy (ARPES), scanning tunneling spectroscopy (STM), and numerical calculations, we demonstrate that the canonical FeSC, Li(Fe,Co)As, is a Hund's superconductor, where the Hundness controls the entire temperature (T) vs doping (x) phase diagram. Our results place strong experimental evidence to support a pairing mechanism driven by the Hundness-induced critical spin fluctuations for the FeSCs [21].

We choose Li(Fe,Co)As for this study as its phase diagram is not intervened by any magnetic or nematic long range orders [22]. This condition is crucial as the Hund's metal physics is essentially a description of the PM phase. Another reason to study Li(Fe,Co)As is that the Hund's coupling induced characteristic orbital differentiation in the dynamical charge and magnetic excitations are observed in the parent compound LiFeAs [17–19].

II. RESULT

We first explore the PM state of electron- and hole-doped LiFeAs via transport measurements (see Supplemental Material [22] and Refs. [23–31] therein for experimental and computational methods). Figure 1(a) shows the normalized resistivity of Li(Fe,TM)As (TM=V, Co) that cover a wide doping range, corresponding to the occupation number, n , from 5.97 to 6.4 [22,32]. For comparison, we also include the normalized resistivity of Ba_{0.6}K_{0.4}Fe₂As₂ (K40) and KFe₂As₂ (K122) that correspond to $n = 5.8$ and 5.5,

*These authors contributed equally to this work.

†miaoh@ornl.gov

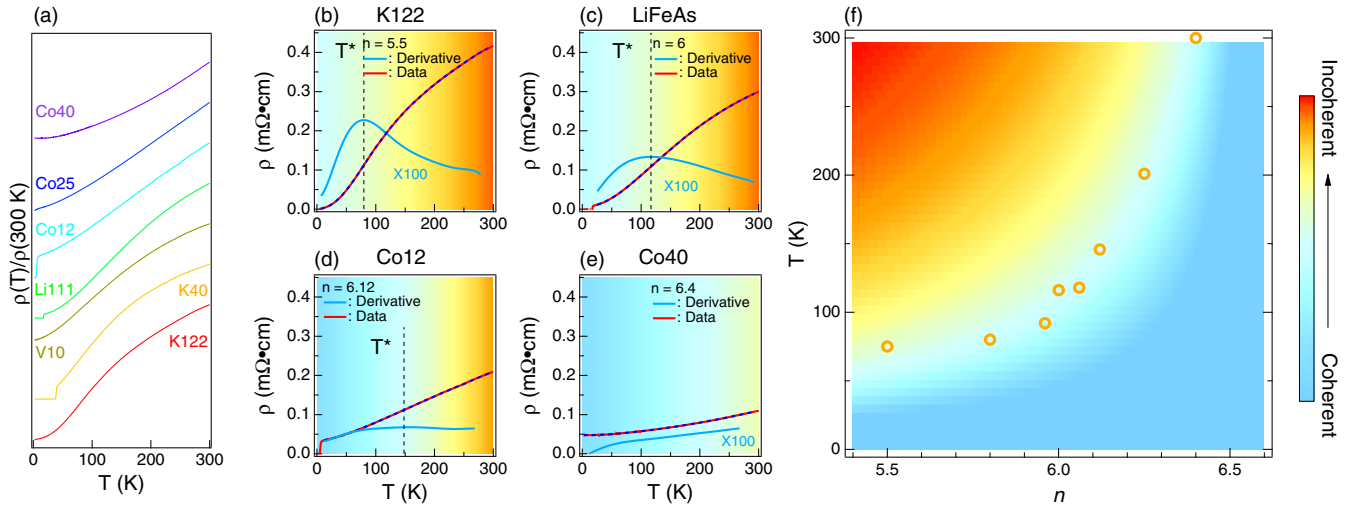


FIG. 1. Doping-dependent coherent-incoherent crossover. (a) Normalized resistivity of $\text{LiFe}_{0.6}\text{Co}_{0.4}\text{As}$ (Co40), $\text{LiFe}_{0.75}\text{Co}_{0.25}\text{As}$ (Co25), $\text{LiFe}_{0.88}\text{Co}_{0.12}\text{As}$ (Co12), LiFeAs (Li111), $\text{LiFe}_{0.9}\text{V}_{0.1}\text{As}$ (V10), $\text{Ba}_{0.6}\text{K}_{0.4}\text{Fe}_2\text{As}_2$ (K40), and KFe_2As_2 (K122). Resistivity (red curve) of K122, LiFeAs, Co12, and Co40 are shown in (b)–(e). Dashed lines are polynomial fittings, $\rho_{\text{FIT}}(T) = \sum_{n=0}^9 a_n T^n$, of the resistivity. Cyan curves in (b)–(e) are the first derivative ($\frac{d\rho_{\text{FIT}}}{dT}$) of the fitted resistivity. The dashed vertical line marks the maximum of $\frac{d\rho_{\text{FIT}}}{dT}$, which is defined as the coherent-incoherent crossover temperature, T^* [8]. The error bars determined by this method are smaller than the symbol size. (f) Extracted n -dependent T^* is remarkably consistent with theoretical predictions for Hund’s metal [7,8,11]. Here n is converted from the Co concentration x (%) [22]. The background colors in (b)–(f) represent the electronic coherence determined by the resistivity curvature.

respectively [33,34]. From the electron-doped side to the hole-doped side, the resistivity curvature undergoes a qualitative change: it remains positive in the entire temperature range in $\text{LiFe}_{0.6}\text{Co}_{0.4}\text{As}$ (Co40) but changes sign at high temperature in LiFeAs. Previous DMFT studies have shown that the curvature change in resistivity represents a coherent-incoherent crossover of the electronic system [8]. To quantify this change, we show the resistivity of K122, LiFeAs, $\text{LiFe}_{0.88}\text{Co}_{0.12}\text{As}$ (Co12), and Co40 in Figs. 1(b)–1(e). First of all, we notice that the room temperature resistivity ρ_{300} decreases by a factor of 4 from K122 to Co40 despite a larger number of impurities in Co40, suggesting reduced electronic interaction via electron doping. We then fit the resistivity curves above T_c with ninth-order polynomial and use the maximum of the first derivative to characterize the coherent-incoherent crossover temperature, T^* [Figs. 1(b)–1(e)]. Figure 1(f) summarizes T^* as a function of n , where the T^* increases from 80 K in K122 to room temperature in Co40, remarkably consistent with previous LDA+DMFT calculations [8,11] and in agreement with our resistivity calculations for LiFeAs (see Supplemental Material [22]).

The evolution of coherent-incoherent crossover in resistivity mirrors the n -dependent electronic interactions. To directly show this trend, we plot the doping-dependent electronic structure measured by ARPES at the Γ and M points in Figs. 2(a)–2(f). The dashed lines are parabolic fittings of the band structure with their colors representing the main orbital characters. Figure 2(g) summarizes the extracted band and orbital-resolved effective mass, m^* , as a function of n . We find that m^* of all bands are reduced by a factor of 2 from LiFeAs to Co40. This is in agreement with the bandwidth evolution of the β band [Fig. 2(h)], which is determined by the energy difference between the top of the β band and the bottom of the γ band.

The profound doping-dependent T^* and m^* strongly indicate that the entire superconducting dome ($6 < n < 6.16$) of $\text{Li}(\text{Fe},\text{Co})\text{As}$ is emerging from the Hund’s metal normal state, where both T^* and m^* are primarily determined by J_H rather than U [8,11,22]. To uncover the Hundness in the superconducting state, we extract the doping-dependent superconducting (SC) gap from scanning tunneling microscopy/spectroscopy (STM/STS) measurements of $\text{Li}(\text{Fe},\text{Co})\text{As}$ at 400 mK, deep in the superconducting state [35]. Figure 3(b) shows a typical atomically resolved STM topography image of $\text{LiFe}_{0.99}\text{Co}_{0.01}\text{As}$. The spatially averaged STS spectra of eight different doping levels with T_c ranging from 18 to 4 K are shown in Fig. 3(a). The dashed lines mark the zero-intensity value for each doping. The extracted Δ_{max} as a function of doping is plotted on top of the T_c vs n diagram in Fig. 3(c). The perfect overlap of these two plots demonstrates a universal $2\Delta_{\text{max}}/k_B T_c \sim 7.7$ scaling in the entire $\text{Li}(\text{Fe},\text{Co})\text{As}$ superconducting phase. This value is nicely consistent with a recent model study, where a universal $2\Delta_{\text{max}}/k_B T_c \sim 7.2$ is derived by assuming the Cooper pairs are “glued” by the Hundness-induced local spin fluctuations with a characteristic $\chi''_{sp}(\omega) \propto \omega^{-6/5}$ scaling [21,22,36]. $\chi''_{sp}(\omega)$ is the imaginary part of the local dynamical susceptibility. The nearly perfect agreement between the theory and experiment in the entire phase diagram firmly establishes the Hund’s superconductivity in $\text{Li}(\text{Fe},\text{Co})\text{As}$.

III. DISCUSSION

Our results have significant implications on the pairing mechanism of FeSCs. Figure 3(d) shows the $2\Delta_{\text{max}}$ vs $k_B T_c$ plot of a large number of FeSCs including $\text{Li}(\text{Fe},\text{Co})\text{As}$. The ubiquitous $2\Delta_{\text{max}}/k_B T_c$ scaling over a large set of FeSCs suggests a common pairing mechanism for all FeSCs.

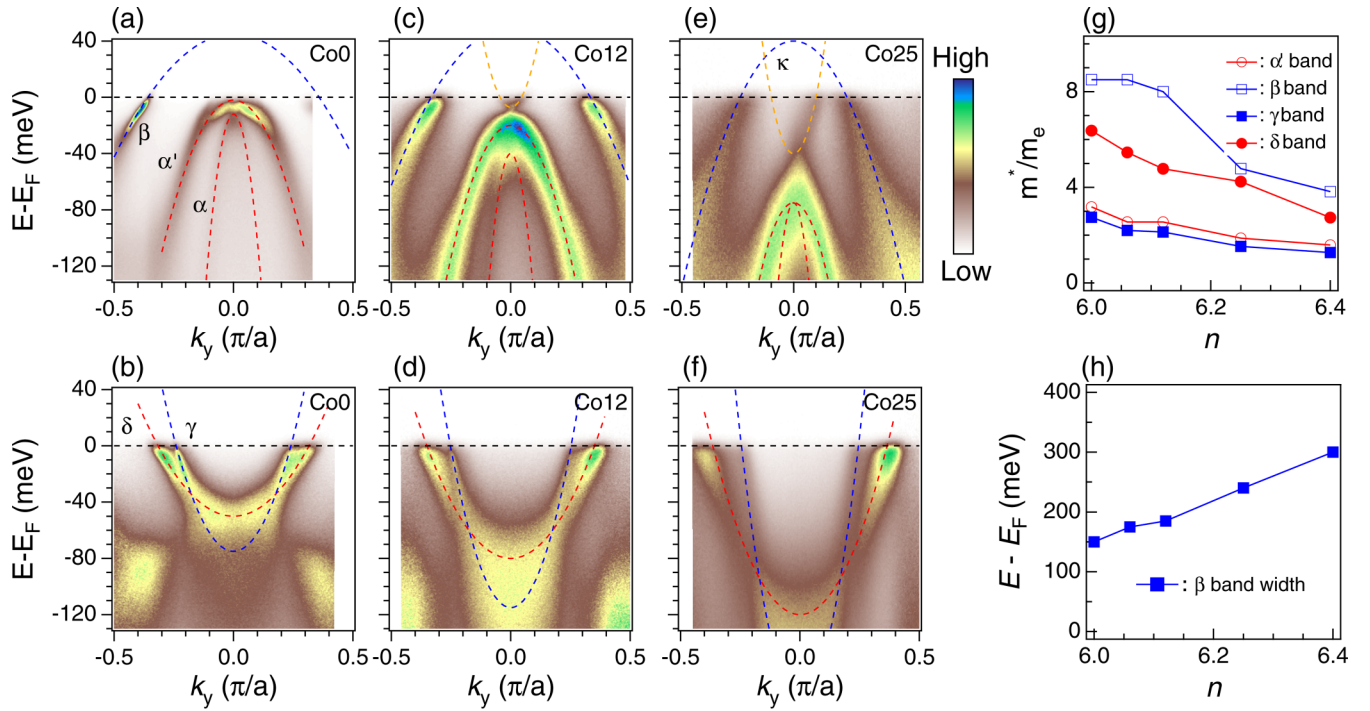


FIG. 2. Doping-dependent band structure of Li(Fe,Co)As. The ARPES intensity plot near the Γ (a)–(c) and M (d)–(f) points. Dashed lines are parabolic fitting of the band dispersion (peak intensity). The extracted doping-dependent effective mass of the α' , β , γ , and δ bands is shown in (g). (h) shows the n -dependent bandwidth of the β band, determined by the band top of the β band and the band bottom of the γ band. Since the β and γ bands are degenerate at the M point, the energy difference between the top of β and the bottom of γ (g) is equivalent to the bandwidth of the β band, which is broadened by a factor of 2 from LiFeAs to Co40, consistent with the doping-dependent effective mass of the β band in (g).

The consistent $2\Delta_{\max}/k_B T_c$ value between the experimental data and model calculation strongly indicates that the leading pairing interaction is the Hundness-induced local spin

fluctuations. This conclusion explains early experimental observations where the SC gap function $\Delta(k)$ follows simple local form factors and involves electronic state away from

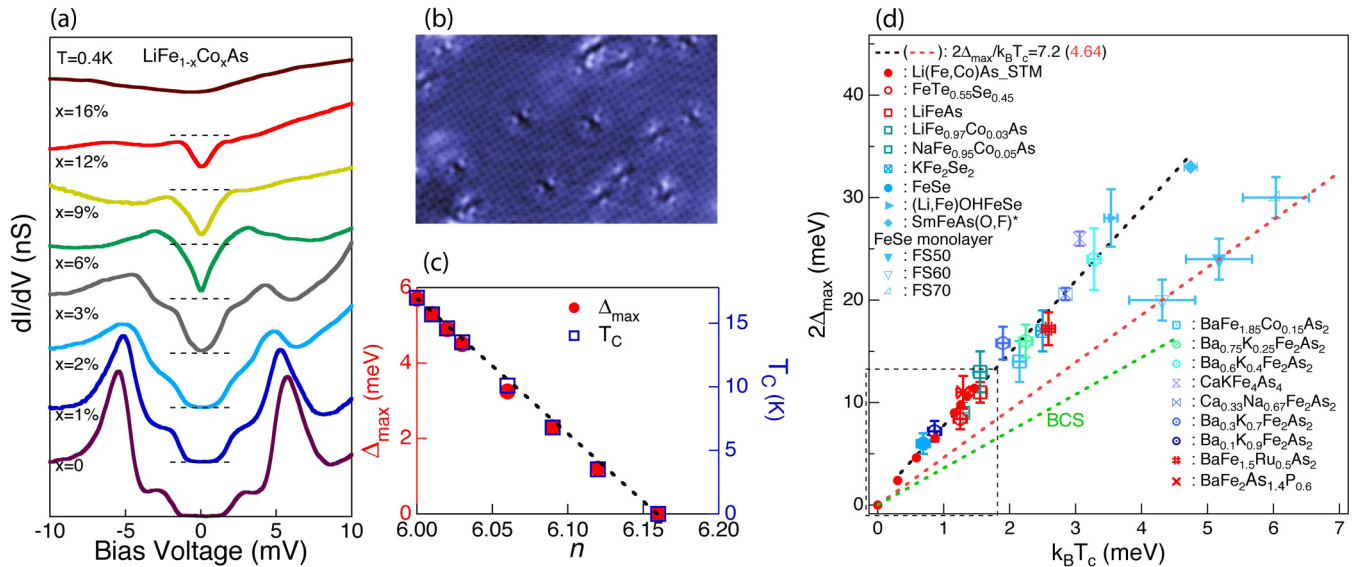


FIG. 3. Doping-dependent SC gap and universal $2\Delta_{\max}/k_B T_c$ scaling. (a) Averaged STS spectra measured at $T = 400$ mK. The dashed lines centered in the zero bias voltage represent zero dI/dV . (b) The STM topography of $\text{LiFe}_{0.99}\text{Co}_{0.01}\text{As}$. (c) The T_c and extracted Δ_{\max} as a function of doping are shown in red circles and blue squares. Data shown in (a) and (c) are adapted from Ref. [35]. (d) shows the universal $2\Delta_{\max}/k_B T_c$ scaling of FeSCs [20]. The black and green dashed lines correspond to Hund's superconductor and BCS superconductor, respectively. The red dashed line is a fit to $2\Delta_{\max}/k_B T_c$ extracted from FeSe monolayer.

the Fermi energy E_F [37–39]. It should be noted, however, the theoretically derived $2\Delta_{\max}/k_B T_c$ is based on a simplified model that neglects several material-specific details such as the proximity to electronic nematicity in $\text{Ba}(\text{Fe},\text{Co})_2\text{As}_2$ and bulk FeSe [40–42] and strong electron-phonon coupling in FeSe monolayer [43]. In addition, the presence of non-local interaction can induce moderate gap variations on the Fermi surface [44–46]. However, the large number of FeSCs with a similar $2\Delta_{\max}/k_B T_c$ ratio suggests that the Hundness is robust even in the presence of various low-energy modifications.

In summary, using transport and spectroscopic techniques, we synergistically uncovered signatures of Hundness from the normal to SC state of $\text{Li}(\text{Fe},\text{Co})\text{As}$. Our result establishes the Hund's superconductivity in canonical FeSC $\text{Li}(\text{Fe},\text{Co})\text{As}$ and indicates that the Hundness-induced critical spin fluctuation is the leading pairing interaction in FeSCs.

ACKNOWLEDGMENTS

This research at Oak Ridge National Laboratory (ORNL) was sponsored by the Laboratory Directed Research and

Development Program of ORNL, managed by UT-Battelle, LLC, under Contract No. DE-AC05-00OR22725 for the US Department of Energy (ARPES) and by the US Department of Energy, Office of Science, Basic Energy Sciences, Materials Sciences and Engineering Division (transport). Y.W. was supported by the US Department of Energy, Office of Science, Basic Energy Sciences as a part of the Computational Materials Science Program through the Center for Computational Design of Functional Strongly Correlated Materials and Theoretical Spectroscopy. G.K. was supported by NSF Grant No. DMR-1733071. Work at the IOP is supported by grants from the National Natural Science Foundation of China (Grants No. 11888101 and No. 11674371), and the Ministry of Science and Technology of China (Grant No. 2016YFA0401000). Work at Princeton University was supported by the Gordon and Betty Moore Foundation (GBMF4547/Hasan) and the US Department of Energy (US DOE) under the Basic Energy Sciences program (Grant No. DOE/BES DE-FG-02-05ER46200). This work is partly based on support by the US DOE, Office of Science through the Quantum Science Center (QSC), a National Quantum Information Science Research Center.

-
- [1] Y. Kamihara, T. Watanabe, M. Hirano, and H. Hosono, *J. Am. Chem. Soc.* **130**, 3296 (2008).
- [2] P. J. Hirschfeld, M. M. Korshunov, and I. I. Mazin, *Rep. Prog. Phys.* **74**, 124508 (2011).
- [3] D. J. Scalapino, *Rev. Mod. Phys.* **84**, 1383 (2012).
- [4] F. C. Zhang and T. M. Rice, *Phys. Rev. B* **37**, 3759 (1988).
- [5] T. Misawa, K. Nakamura, and M. Imada, *Phys. Rev. Lett.* **108**, 177007 (2012).
- [6] H. Ikeda, R. Arita, and J. Kuneš, *Phys. Rev. B* **82**, 024508 (2010).
- [7] P. Werner, E. Gull, M. Troyer, and A. J. Millis, *Phys. Rev. Lett.* **101**, 166405 (2008).
- [8] K. Haule and G. Kotliar, *New J. Phys.* **11**, 025021 (2009).
- [9] Z. P. Yin, K. Haule, and G. Kotliar, *Nat. Mater.* **10**, 932 (2011).
- [10] Z. P. Yin, K. Haule, and G. Kotliar, *Nat. Phys.* **7**, 294 (2011).
- [11] P. Werner, M. Casula, T. Miyake, F. Aryasetiawan, A. J. Millis, and S. Biermann, *Nat. Phys.* **8**, 331 (2012).
- [12] A. Georges, L. de' Medici, and J. Mravlje, *Annu. Rev. Condens. Matter Phys.* **4**, 137 (2013).
- [13] L. de' Medici, G. Giovannetti, and M. Capone, *Phys. Rev. Lett.* **112**, 177001 (2014).
- [14] K. M. Stadler, Z. P. Yin, J. von Delft, G. Kotliar, and A. Weichselbaum, *Phys. Rev. Lett.* **115**, 136401 (2015).
- [15] E. Walter, K. M. Stadler, S.-S. B. Lee, Y. Wang, G. Kotliar, A. Weichselbaum, and J. von Delft, *Phys. Rev. X* **10**, 031052 (2020).
- [16] M. Yi, D. H. Lu, R. Yu, S. C. Riggs, J.-H. Chu, B. Lv, Z. K. Liu, M. Lu, Y.-T. Cui, M. Hashimoto, S.-K. Mo, Z. Hussain, C. W. Chu, I. R. Fisher, Q. Si, and Z.-X. Shen, *Phys. Rev. Lett.* **110**, 067003 (2013).
- [17] H. Miao, Z. P. Yin, S. F. Wu, J. M. Li, J. Ma, B.-Q. Lv, X. P. Wang, T. Qian, P. Richard, L.-Y. Xing, X.-C. Wang, C. Q. Jin, K. Haule, G. Kotliar, and H. Ding, *Phys. Rev. B* **94**, 201109(R) (2016).
- [18] Z. P. Yin, K. Haule, and G. Kotliar, *Nat. Phys.* **10**, 845 (2014).
- [19] Y. Li, Z. Yin, X. Wang, D. W. Tam, D. L. Abernathy, A. Podlesnyak, C. Zhang, M. Wang, L. Xing, C. Jin, K. Haule, G. Kotliar, T. A. Maier, and P. Dai, *Phys. Rev. Lett.* **116**, 247001 (2016).
- [20] H. Miao, W. H. Brito, Z. P. Yin, R. D. Zhong, G. D. Gu, P. D. Johnson, M. P. M. Dean, S. Choi, G. Kotliar, W. Ku, X. C. Wang, C. Q. Jin, S.-F. Wu, T. Qian, and H. Ding, *Phys. Rev. B* **98**, 020502(R) (2018).
- [21] T.-H. Lee, A. Chubukov, H. Miao, and G. Kotliar, *Phys. Rev. Lett.* **121**, 187003 (2018).
- [22] See Supplemental Material at <http://link.aps.org/supplemental/10.1103/PhysRevB.103.054503> for experimental method and DFT+DMFT calculation of resistivity.
- [23] K. Haule, C.-H. Yee, and K. Kim, *Phys. Rev. B* **81**, 195107 (2010).
- [24] P. Blaha, K. Schwarz, F. Tran, R. Laskowski, G. K. H. Madsen, and L. D. Marks, *J. Chem. Phys.* **152**, 74101 (2020).
- [25] E. Gull, A. J. Millis, A. I. Lichtenstein, A. N. Rubtsov, M. Troyer, and P. Werner, *Rev. Mod. Phys.* **83**, 349 (2011).
- [26] X. C. Wang, Q. Q. Liu, Y. X. Lv, W. B. Gao, L. X. Yang, R. C. Yu, F. Y. Li, and C. Q. Jin, *Solid State Commun.* **148**, 538 (2008).
- [27] A. Kutepov, K. Haule, S. Y. Savrasov, and G. Kotliar, *Phys. Rev. B* **82**, 045105 (2010).
- [28] X. Deng, K. Haule, and G. Kotliar, *Phys. Rev. Lett.* **116**, 256401 (2016).
- [29] Y. M. Dai, H. Miao, L. Y. Xing, X. C. Wang, P. S. Wang, H. Xiao, T. Qian, P. Richard, X. G. Qiu, W. Yu, C. Q. Jin, Z.

- Wang, P. D. Johnson, C. C. Homes, and H. Ding, *Phys. Rev. X* **5**, 031035 (2015).
- [30] L. Y. Xing, X. Shi, P. Richard, X. C. Wang, Q. Q. Liu, B. Q. Lv, J.-Z. Ma, B. B. Fu, L.-Y. Kong, H. Miao, T. Qian, T. K. Kim, M. Hoesch, H. Ding, and C. Q. Jin, *Phys. Rev. B* **94**, 094524 (2016).
- [31] X.-P. Wang, P. Richard, Y.-B. Huang, H. Miao, L. Cevey, N. Xu, Y.-J. Sun, T. Qian, Y.-M. Xu, M. Shi, J.-P. Hu, X. Dai, and H. Ding, *Phys. Rev. B* **85**, 214518 (2012).
- [32] X. Shi, Z.-Q. Han, X.-L. Peng, P. Richard, T. Qian, X.-X. Wu, M.-W. Qiu, S. C. Wang, J. P. Hu, Y.-J. Sun, and H. Ding, *Nat. Commun.* **8**, 14988 (2017).
- [33] H. Ding, P. Richard, K. Nakayama, K. Sugawara, T. Arakane, Y. Sekiba, A. Takayama, S. Souma, T. Sato, T. Takahashi, Z. Wang, X. Dai, Z. Fang, G. F. Chen, J. L. Luo, and N. L. Wang, *Europhys. Lett.* **83**, 47001 (2008).
- [34] D. Fang, X. Shi, Z. Du, P. Richard, H. Yang, X. X. Wu, P. Zhang, T. Qian, X. Ding, Z. Wang, T. K. Kim, M. Hoesch, A. Wang, X. Chen, J. Hu, H. Ding, and H.-H. Wen, *Phys. Rev. B* **92**, 144513 (2015).
- [35] J.-X. Yin, S. S. Zhang, G. Dai, Y. Zhao, A. Kreisel, G. Macam, X. Wu, H. Miao, Z.-Q. Huang, J. H. J. Martiny, B. M. Andersen, N. Shumiya, D. Multer, M. Litskevich, Z. Cheng, X. Yang, T. A. Cochran, G. Chang, I. Belopolski, L. Xing *et al.*, *Phys. Rev. Lett.* **123**, 217004 (2019).
- [36] Y. Wang, E. Walter, S.-S. B. Lee, K. M. Stadler, J. von Delft, A. Weichselbaum, and G. Kotliar, *Phys. Rev. Lett.* **124**, 136406 (2020).
- [37] H. Miao, P. Richard, Y. Tanaka, K. Nakayama, T. Qian, K. Umezawa, T. Sato, Y.-M. Xu, Y. B. Shi, N. Xu, X.-P. Wang, P. Zhang, H.-B. Yang, Z.-J. Xu, J. S. Wen, G.-D. Gu, X. Dai, J.-P. Hu, T. Takahashi, and H. Ding, *Phys. Rev. B* **85**, 094506 (2012).
- [38] J. Hu and H. Ding, *Sci. Rep.* **2**, 381 (2012).
- [39] H. Miao, T. Qian, X. Shi, P. Richard, T. K. Kim, M. Hoesch, L. Y. Xing, X.-C. Wang, C.-Q. Jin, J.-P. Hu, and H. Ding, *Nat. Commun.* **6**, 6056 (2015).
- [40] M. Yi, D. Lu, J.-H. Chu, J. G. Analytis, A. P. Sorini, A. F. Kemper, B. Moritz, S.-K. Mo, R. G. Moore, M. Hashimoto, W.-S. Lee, Z. Hussain, T. P. Devereaux, I. R. Fisher, and Z.-X. Shen, *Proc. Natl. Acad. Sci. USA* **108**, 6878 (2011).
- [41] R. M. Fernandes, A. V. Chubukov, and J. Schmalian, *Nat. Phys.* **10**, 97 (2014).
- [42] P. O. Sprau, A. Kostin, A. Kreisel, A. E. Böhmer, V. Taufour, P. C. Canfield, S. Mukherjee, P. J. Hirschfeld, B. M. Andersen, and J. C. S. Davis, *Science* **357**, 75 (2017).
- [43] J. J. Lee, F. T. Schmitt, R. G. Moore, S. Johnston, Y.-T. Cui, W. Li, M. Yi, Z. K. Liu, M. Hashimoto, Y. Zhang, D. H. Lu, T. P. Devereaux, D.-H. Lee, and Z.-X. Shen, *Nature (London)* **515**, 245 (2014).
- [44] K. Umezawa, Y. Li, H. Miao, K. Nakayama, Z.-H. Liu, P. Richard, T. Sato, J. B. He, D.-M. Wang, G. F. Chen, H. Ding, T. Takahashi, and S.-C. Wang, *Phys. Rev. Lett.* **108**, 037002 (2012).
- [45] S. V. Borisenko, V. B. Zabolotnyy, D. V. Evtushinsky, T. K. Kim, I. V. Morozov, A. N. Yaresko, A. A. Kordyuk, G. Behr, A. Vasiliev, R. Follath, and B. Büchner, *Phys. Rev. Lett.* **105**, 067002 (2010).
- [46] S. Bhattacharyya, K. Björnson, K. Zantout, D. Steffensen, L. Fanfarillo, A. Kreisel, R. Valentí, B. M. Andersen, and P. J. Hirschfeld, *Phys. Rev. B* **102**, 035109 (2020).